

# All-fiber optical filter with an ultranarrow and rectangular spectral response

Xihua Zou,<sup>1,2,3,4,\*</sup> Ming Li,<sup>2,5</sup> Wei Pan,<sup>1</sup> Lianshan Yan,<sup>1</sup> José Azaña,<sup>2</sup> and Jianping Yao<sup>4</sup>

<sup>1</sup>Center for Information Photonics and Communications, Southwest Jiaotong University, Chengdu, 610031, China

<sup>2</sup>Institut National de la Recherche Scientifique—Energie, Matériaux et Télécommunications (INRS-EMT), Québec, Canada

<sup>3</sup>Science and Technology on Electronic Information Control Laboratory, Chengdu 610036, China

<sup>4</sup>Microwave Photonics Research Laboratory, University of Ottawa, Ottawa, K1N 6N5, Canada.

<sup>5</sup>State Key Laboratory on Integrated Optoelectronics, Institute of Semiconductors, CAS, Beijing, China

\*Corresponding author: zouxihua@swjtu.edu.cn

Received March 15, 2013; revised July 10, 2013; accepted July 22, 2013;

posted July 23, 2013 (Doc. ID 187178); published August 13, 2013

Optical filters with an ultranarrow and rectangular spectral response are highly desired for high-resolution optical/electrical signal processing. An all-fiber optical filter based on a fiber Bragg grating with a large number of phase shifts is designed and fabricated. The measured spectral response shows a 3 dB bandwidth of 650 MHz and a rectangular shape factor of 0.513 at the 25 dB bandwidth. This is the narrowest rectangular bandpass response ever reported for an all-fiber filter, to the best of our knowledge. The filter has also the intrinsic advantages of an all-fiber implementation. © 2013 Optical Society of America

OCIS codes: (230.7408) Wavelength filtering devices; (070.2615) Frequency filtering; (060.3735) Fiber Bragg gratings.  
<http://dx.doi.org/10.1364/OL.38.003096>

Optical filters provide fundamental functions for signal processing in a variety of fields. For advanced applications in wireless, optical, quantum communications, radar, lidar, and astronomy systems, a bandpass optical filter with an ultranarrow bandwidth from several GHz down to the MHz range, comparable to that of a conventional electrical filter, is highly desired [1–3]. An optical filter also offers some critical advantages as compared with an electronic solution, such as high operation frequency, large spontaneous bandwidth, low frequency-dependent loss, and strong immunity to electromagnetic interference. However, a key challenge in the design and fabrication of the optical filter is to achieve a spectral response with both an ultranarrow bandwidth and a rectangular spectral profile.

Fiber Bragg gratings (FBGs) have been widely used to implement versatile optical filters [4,5], with advantageous features including flexible spectral response, low insertion loss, and an all-fiber configuration that is fully compatible with other fiber-optic components and systems. FBGs developed for optical communications [6] usually have a bandwidth in the order of tens of GHz or, more typically, exceeding 100 GHz. However, special designs can be employed to implement an FBG with a 3 dB bandwidth of a few GHz or lower by using grating apodization or phase-shift techniques. An FBG with a 3 dB bandwidth of ~5 GHz [7,8] has been demonstrated by properly engineering the grating apodization profile. On the other hand, the phase-shift technique has widely been employed for the design of a volume or fiber grating with an even narrower bandwidth [9–15]. For example, a phase-shifted FBG (PS-FBG) with a 3 dB bandwidth around 2 GHz has been employed to implement multiple-wavelength fiber lasers, single sideband modulation, and microwave channelization [10–12]. A PS-FBG with a bandwidth as low as 100 MHz or 62.5 MHz (i.e., 0.5 pm) has also been reported [13,14]. Based on the equivalent phase shift technique, a PS-FBG with an ultranarrow bandwidth of 2.5 MHz was demonstrated [15].

Although an ultranarrow bandwidth can be achieved in a filter based on an FBG, a Lorentzian or quasi-Lorentzian profile [9–15] with a shape factor of 0.0562 is usually deduced for spectral responses. Here, the shape factor is defined as the ratio between the 3 dB and the 25 dB bandwidths [16]. Generally, an excellent rectangular profile is obtained when this factor is greater than 0.5. However, for many applications, such as RF channelization, a rectangular spectral response is needed. A filter with a rectangular spectral response has other important advantages, such as a more stable and robust filtering processing, higher spectral efficiency, increased spectral sidelobe suppression, lower intrachannel cross-interference, and reduced signal distortions. Multiple phase shifts have been introduced to a grating structure, in the past, to improve the flatness of the spectral response [17–19]. In 2009, we fabricated an flat-top FBG-based filter with a bandwidth of ~5.5 GHz (44 pm) and in-band ripples less than 0.05 dB [20]. The flatness was improved but the spectral response was still far from a rectangular profile.

In this letter, an expected all-fiber optical filter based on an FBG is designed and fabricated. The feature of the filter design is the balanced combination of a large number of phase shifts, a large length, and a weak refractive index perturbation in an FBG to ensure an ultranarrow and rectangular spectral response. More importantly, such a filter with a 3 dB bandwidth of 650 MHz and a rectangular shape factor of 0.513 is experimentally demonstrated for the first time. As other interesting practical advantages, the filter operates in transmission with simple interconnection and low loss, in contrast to conventional FBG filters used in reflection.

As shown in Fig. 1, the designed FBG-based filter has a large number of phase shifts in the refractive index perturbation. Mathematically, when  $N$  phase shifts are inserted, the optical filter is divided into  $N + 1$  grating sections, which can be regarded as a cascade of  $N$  equivalent cavities with coupling effects among them. Using

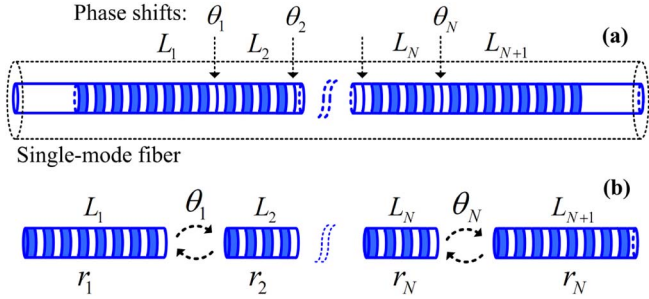


Fig. 1. (a) Configuration of the optical filter and (b) its equivalent coupled-cavity model.

the transfer matrix method, the spectral responses of the device can be calculated as

$$\begin{bmatrix} 1/t \\ r/t \end{bmatrix} = \prod_{i=1}^N \underbrace{\begin{bmatrix} 1/t_i & (r_i/t_i)^* \\ r_i/t_i & (1/t_i)^* \end{bmatrix}}_{L_i} \times \underbrace{\begin{bmatrix} e^{-j\theta_i/2} & 0 \\ 0 & e^{j\theta_i/2} \end{bmatrix}}_{\theta_i} \times \underbrace{\begin{bmatrix} 1/t_{N+1} & (r_{N+1}/t_{N+1})^* \\ r_{N+1}/t_{N+1} & (1/t_{N+1})^* \end{bmatrix}}_{L_{N+1}} \times \begin{bmatrix} 1 \\ 0 \end{bmatrix}, \quad (1)$$

where  $r$  and  $t$  are the complex-field transmission and reflection coefficients of the filter;  $r_i$ ,  $t_i$ , and  $L_i$  are the complex-field reflection and transmission coefficients and the length of  $i$ -th grating section ( $1 \leq i \leq N+1$ ), respectively;  $\theta_i$  is the  $i$ -th phase shift ( $1 \leq i \leq N$ ); and  $*$  represents the complex conjugation. We use a symmetric distribution of multiple  $\pi$  phase shifts, and in particular

$$L_i = L_{N+1-i}, \quad \theta_1 = \theta_2 = \dots = \theta_N = \pi. \quad (2)$$

To minimize the sidelobes in the transmission spectral response, a Gaussian apodization on the refractive index perturbation is also introduced. The specific physical parameters of the designed filter are listed in Table 1. Here, a large length and a weak refractive index perturbation are used to provide a narrow reflection bandwidth. Next, a double-digit number of phase shifts are distributed, with balanced couplings among the equivalent cavities, to generate a narrower and rectangular passband in the narrow reflection bandwidth. Thus an ultranarrow and rectangular spectral response in transmission will result.

The spectral response ( $T = |t|^2$ ) in transmission is numerically calculated using the transfer matrix method [21]. As shown in Fig. 2, a 3 dB bandwidth of 600 MHz, a 25 dB bandwidth of 1270 MHz, a stop-band bandwidth of 30 GHz, and an insertion loss less than

**Table 1. Physical Parameters of the Designed Filter**

| Maximum Perturbation       | Number of Phase Shifts               | Apodization | Length   |
|----------------------------|--------------------------------------|-------------|----------|
| $2.1 \times 10^{-4}$       | 10                                   | Gaussian    | 92.19 mm |
| Length of grating sections | 3.157 7.635 9.47 10.161 10.42 10.506 |             |          |
|                            | 10.42 10.161 9.47 7.635 3.157        |             |          |

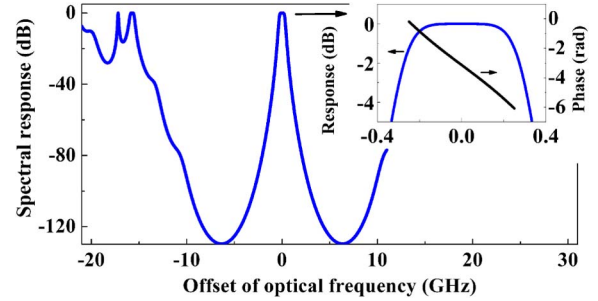


Fig. 2. Numerically simulated spectral response of the filter.

1 dB are expected, leading to a shape factor of 0.5. Therefore, the designed all-fiber optical filter has both an ultranarrow bandwidth and an excellent rectangular profile. In addition to the amplitude response, a quasi-linear phase response is also observed in the passband.

The designed optical filter is then fabricated in a standard single-mode fiber by using a phase mask with a uniform pitch of 1070.4 nm through UV exposure at 244 nm. The implementations of the Gaussian apodization and the phase shifts are key steps for fabrication. The Gaussian apodization in refractive index perturbation is formed through controlling the scanning speed of the UV beam along the fiber, and a maximum perturbation is estimated to be  $\sim 2.1 \times 10^{-4}$ . There are a total of 10 phase shifts in the 92.192-mm filter and each phase shift is introduced by using a nanopositioning stage to move the phase mask by a quarter-pitch displacement.

To evaluate the spectral response of the fabricated filter, two measurement methods are employed. The first one is performed in the optical domain by use of an optical vector network analyzer (OVNA, LUNA OVA-5000). Since an OVNA has a wavelength scanning range up to 75 nm, this feature is employed to characterize the spectral response over a large wavelength range. To have a spectral response measurement with a higher resolution of  $\sim$ MHz, we also measure the spectral response in the electrical domain using an electrical VNA (EVNA, Agilent N5230A). The measurement configuration using an EVNA is shown in Fig. 3. The spectral response of the filter can be derived from the beating between the optical carrier from the upper path and the filtered +1 st sideband from the lower path, under the frequency-scanning mode of the EVNA.

Figure 4(a) shows a full view of the spectral response measured by the OVNA, where the measurement resolution is  $\sim$ 160 MHz. A stop-band bandwidth of 30.4 GHz

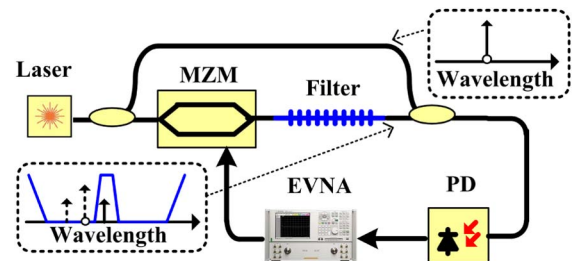


Fig. 3. Measurement configuration in the electrical domain. MZM, Mach-Zehnder modulator; PD, photodetector; EVNA, electrical vector network analyzer.

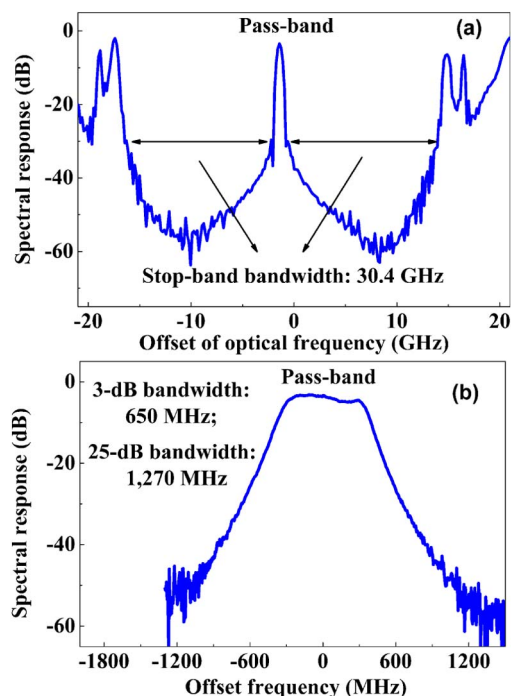


Fig. 4. (a) Full view of the spectral response measured by the OVNA and (b) a zoom-in view of the passband with a resolution of 6 MHz, measured by the EVNA. (The different signal levels of stop band at corresponding offset frequencies in (a) and (b) mainly arise from the two different measurement methods used to obtain each plot.)

**Table 2. Measured Specifications of the Optical Filter**

| Specifications      | Values       |
|---------------------|--------------|
| 3 dB bandwidth      | 650 MHz      |
| 25 dB bandwidth     | 1270 MHz     |
| Shape factor        | 0.513        |
| Stop-band bandwidth | 30.4 GHz     |
| Insertion loss      | 3 dB         |
| Rejection ratio     | 50 dB        |
| Ripples             | $\pm 0.7$ dB |
| Central wavelength  | 1548.046 nm  |

is achieved. The spectral response of the passband, measured with a higher resolution of 6 MHz using the EVNA, is shown in Fig. 4(b). As can be seen, the filter has a 3 dB bandwidth of 650 MHz and a 25 dB bandwidth of 1270 MHz. Thus, the rectangular shape factor is calculated to be 0.513. More specifications of the fabricated filter, including the insertion loss, the out-of-band rejection ratio, the in-band ripples, and the central wavelength, are provided in Table 2, while the quasi-linear phase response is not presented due to the limit of the measurement configurations. The key requirements (an ultranarrow bandwidth and an excellent shape factor) are fulfilled.

In conclusion, an all-fiber optical filter with an ultranarrow and rectangular spectral response was designed and fabricated on a single-mode fiber. The measured spectral responses showed that the filter had an ultranarrow 3 dB bandwidth of 650 MHz and a rectangular shape factor of 0.513. In addition, the filter also exhibited an insertion loss of only 3 dB, a stop-band bandwidth of 30.4 GHz, and a rejection ratio of 50 dB. To the best of our knowledge, this is the first demonstration of an all-fiber filter with both an extremely ultranarrow bandwidth and an excellent rectangular profile in the bandpass response.

The work was supported by the National Natural Science Foundation of China (61101053), the “973” Project (2012CB315704), the Program for New Century Excellent Talents in University of China (NCE-12-0940), the Fund of Science and Technology on Electronic Information Control Laboratory, and the Natural Science and Engineering Research Council of Canada (NSERC).

## References

- W. Horn, S. Kroesen, and C. Denz, *Appl. Phys. Lett.* **98**, 241116 (2011).
- Y. Wang, S. Zhang, D. Wang, Z. Tao, Y. Hong, and J. Chen, *Opt. Lett.* **37**, 4059 (2012).
- D. Sáez-Rodríguez, J. L. Cruz, A. Díez, and M. V. Andrés, *Opt. Lett.* **37**, 4314 (2012).
- K. O. Hill, Y. Fujii, D. C. Johnson, and B. S. Kawasaki, *Appl. Phys. Lett.* **32**, 647 (1978).
- G. Meltz, M. M. Morey, and W. H. Glenn, *Opt. Lett.* **14**, 823 (1989).
- C. R. Giles, *J. Lightwave Technol.* **15**, 1391 (1997).
- L. Zhang, K. Sugden, I. Bennion, and A. Mology, *Electron. Lett.* **31**, 477 (1995).
- T. Komukai, K. Tamura, and M. Nakazawa, *IEEE Photon. Technol. Lett.* **9**, 934 (1997).
- G. P. Agrawal and S. Radic, *IEEE Photon. Technol. Lett.* **6**, 995 (1994).
- L. Xia, P. Shum, Y. Wang, and T. H. Cheng, *IEEE Photon. Technol. Lett.* **18**, 2162 (2006).
- D. B. Hunter, L. G. Edvell, and M. A. Englund, in *Proceedings of 2005 IEEE International Topical Meeting on Microwave Photonics*, (IEEE, 2005), pp. 249–251.
- S. R. Blais and J. P. Yao, *IEEE Photon. Technol. Lett.* **18**, 2230 (2006).
- J. Canning and M. G. Sceats, *Electron. Lett.* **30**, 1344 (1994).
- X. M. Liu, *Opt. Commun.* **280**, 147 (2007).
- X. F. Chen, J. P. Yao, F. Zeng, and Z. Deng, *IEEE Photon. Technol. Lett.* **17**, 1390 (2005).
- B. E. Little, S. T. Chu, P. P. Absil, J. V. Hryniewicz, F. G. Johnson, F. Seiferth, D. Gill, V. Van, O. King, and M. Trakalo, *IEEE Photon. Technol. Lett.* **16**, 2263 (2004).
- R. Zengerle and O. Leminger, *J. Lightwave Technol.* **13**, 2354 (1995).
- F. Bakhti and P. Sansonetti, *J. Lightwave Technol.* **15**, 1433 (1997).
- L. Wei and J. W. Y. Lit, *J. Lightwave Technol.* **15**, 1405 (1997).
- X. Zou, F. Wang, and W. Pan, *Appl. Opt.* **48**, 691 (2009).
- T. Erdogan, *J. Lightwave Technol.* **15**, 1277 (1997).